Histone deacetylases regulate organ-specific growth in a horned beetle

Authors:

Yonggang Hu[1,2 *], Jordan R. Crabtree[1], Anna L. M. Macagno[1,3], Armin P. Moczek[1]

Affiliations:

[1] Department of Biology, Indiana University, 915 East 3rd Street, Bloomington, IN 47405, USA

[2] State Key Laboratory of Resource Insects, Institute of Sericulture and Systems Biology, Southwest University, Chongqing, 400715, China

[3] Biostatistics Consulting Center, Department of Epidemiology and Biostatistics, School of Public Health Bloomington, Indiana University, 2719 E. 10th Street, Bloomington, IN 47405, USA

* corresponding author details:
State Key Laboratory of Resource Insects, Institute of Sericulture and Systems Biology, Southwest University, Chongqing, 400715, China
email: yongganghu@swu.edu.cn

Short running title: HDAC function in horned beetle development

Keywords: *Onthophagus*, chromatin, plasticity, nutrition

Abstract

Nutrient availability is among the most widespread means by which environmental variability affects developmental outcomes. Because almost all cells within an individual organism share the same genome, structure-specific growth responses must result from changes in gene regulation. Earlier work suggested that *histone deacetylases* (*HDACs*) may serve as epigenetic regulators linking nutritional conditions to trait-specific development. Here we assess the function of diverse histone deacetylases in the structure-specific growth of both sex-shared and sex-specific traits including evolutionarily novel structures in the horned dung beetle *Onthophagus taurus*. We identified five *HDAC* members whose down-regulation yielded highly variable mortality depending on which *HDAC* member was targeted. We then show that most *HDAC* members operate in both a gene- and trait-specific manner in the regulation of nutrition-responsiveness of appendage size and shape. Most importantly, we find that *HDACs* pattern the morphology and regulate the scaling of evolutionarily novel head and thoracic horns as a function of nutritional variation. Collectively, our results suggest that both functional overlap and division of labor among *HDAC* members contribute to morphological diversification of both conventional and recently evolved appendages. More generally, our work raises the possibility that *HDAC*-mediated scaling relationships and their evolution may underpin morphological diversification within and across insect species broadly.

INTRODUCTION

Phenotypic plasticity is the ability of an organism to change its phenotype in response to environmental stimuli (Schlichting and Pigliucci 1998; West-Eberhard 2003), a universal phenomenon in the living world. Diverse abiotic (e.g. temperature, photoperiod) and biotic (e.g. conspecific density) may influence growth and differentiation (Régnière et al., 2012; Prudic et al., 2011; O'Leary et al., 2017). Among those, nutrition is one of the most widespread means by which environmental variability affects developmental outcomes. Lack of essential nutrients can slow or arrest development, and sometimes trigger alternative developmental programs, such as the diapause of insects and worms (Lafuente and Beldade 2019). Nutrition also serves as a major determinant of animal size and shape (Andersen et al. 2013; Rohner et al. 2022), with poor nutrition generally yielding reduced growth and final adult body size in animals with determinate growth such as insects and mammals. However, different body parts within an individual typically differ in their response to nutrient availability. For instance, brain size in mammals and male genital size in arthropods are relatively nutrition-insensitive (Koh et al. 2005; Eberhard 2009), whereas secondary sexual traits such as male horns of dung and rhinoceros beetles (Moczek 1998; Ito et al. 2013), or mandibles of stag and broad-horned flour beetles (Gotoh et al. 2014; Okada et al. 2019) are exquisitely sensitive to nutritional variation during development. Such trait-specific scaling relationships therefore contribute in important ways to shape morphological diversity within and among taxa. Here we investigate the role of epigenetic modifications via organ-specific growth responses in an insect model.

Because all cells within an individual organism essentially share the same genome, organ- or structure-specific growth must result from changes in gene regulation. Much recent work has described changes in transcription profiles in response to environmental modifications such as nutrient availability, and has begun to identify key regulators of condition-responsive growth (e.g., *insulin*/*IIS* (Emlen et al. 2012; Snell-Rood and Moczek 2012; Xu et al. 2015), *doublesex* (Kijimoto et al. 2012), and *hedgehog* (Kijimoto and Moczek 2016)). However, how such differential expression is achieved in the first place, and then subsequently transduced into organ-specific growth is much less well understood. Here we investigate the role of epigenetic modifications in enabling organ-specific growth, with a particular emphasis on histone modifications. Histone acetylation/deacetylation is crucial in the organization of euchromatin (which enables transcription) and heterochromatin (which inhibits transcription), thereby mediating differential gene expression. Histone deacetylases (HDACs) are members of an ancient enzyme family that reverses the acetylation of protein substrates. *HDAC*-mediated

removal of acetylation from histone tail lysines generally correlates with gene silencing by decreasing the ability of transcription factors to access DNA (Chen et al. 2015). In insects, studies have confirmed that *HDACs* play a role in various developmental processes, such as growth (Ozawa et al. 2016), metamorphosis (George et al. 2019; George and Palli 2020a; George and Palli 2020b), long-term memory (Fitzsimons et al. 2013), reproduction (Zhang et al. 2018), longevity (Frankel et al. 2015), caste differentiation (Spannhoff et al. 2011; Suzuki et al. 2019), diapause (Cui et al. 2022), and immunity (Mukherjee et al. 2012). Furthermore, in the broad-horned flour beetle *Gnatocerus cornutus*, *HDAC1* and *HDAC3* differentially participate in the nutrition-dependent growth of wings and male-exaggerated mandibles, suggesting that *HDACs* may serve as epigenetic regulators linking nutritional conditions to trait-specific development (Ozawa et al. 2016). Here we expand on this work by assessing the function of diverse histone deacetylases in the structure-specific growth of both sex-shared and sex-specific traits including evolutionarily novel structures in a horned dung beetle.

Horned dung beetles (genus *Onthophagus*) have emerged as promising model systems to investigate the development and diversification of scaling relationships. Here we employ one such model, the bull-headed dung beetle *O. taurus*, to investigate the function of five different *HDAC* members in the development of four different morphological structures. We selected hind legs as examples of traits that exhibit moderate nutrition-responsiveness and therefore scale roughly isometrically with body size. We also investigated male genitalia because of their relatively muted nutrition response and corresponding hypoallometric scaling. Finally, we assessed thoracic horns and head horns because of their highly sex-specific growth and scaling relationships (Casasa et al. 2017). Thoracic horns are observed only in the pupal stage of both sexes where they function as molting devices in the shedding of the larval head capsule during the larval-pupal molt, and exhibit exaggerated growth in males (Moczek et al. 2006; Moczek 2006). In partial contrast, head horns are found only in male pupae and adults and exhibit extreme nutrition-responsive growth resulting in hyper-allometric scaling with body size. Head horns function as weapons in competition between adult males over reproductive access to females. While thoracic horns have recently been identified as partial wing serial homologs (Hu et al. 2019), head horns lack any obvious homology with other structures and are thus considered evolutionary novelties even by the strictest of definitions (Müller and Wagner 1991; Moczek 2005). Below we detail our results and discuss them in the light of the developmental regulation of growth and plasticity in horned beetles in particular and insects broadly.

RESULTS AND DISCUSSION

We sought to characterize the presence and function of *HDACs* during the development of the bull-headed dung beetle *O. taurus*. We identified five *HDACs* in the annotated genome, which based on phylogenetic analysis could be classified into three classes: class I (*HDAC1* and *HDAC3*), class II (*HDAC4* and *HDAC6*), and class IV (*HDAC11*) (Fig. S1). We then performed RNAi experiments by injecting double-stranded RNA (dsRNA) corresponding to each of the five HDACs into newly molted final-instar *O. taurus* larvae and assessed their influence on pupal and adult morphologies. Wildtype morphology for each focal phenotype is shown in Figure 1.

HDAC-RNAi resulted in highly variable mortality depending on target *HDAC*

RNAi-mediated knockdown of *HDAC1* resulted in 100% larval mortality at the initial 1 µg/µl dsRNA injection dosage, as well as subsequent dosages as low as 0.25 µg/µl (Table S1). Most larvae exhibited arrested development at the pre-pupal stages and eventually died with larval-pupal intermediate phenotypes with pupal traits, such as compound eyes, observed underneath the larval integument. A mass of fat body accumulated underneath the posterior region of the developing pupal abdomen, resulting in a cavity filled with hemolymph between the larval integument and newly-formed pupal cuticle (Fig. 2A and B). These results are in line with previous studies in *Tribolium castaneum* (George et al. 2019), which suggest that *HDAC1* expression is required for suppressing the juvenile hormone (JH) response gene *Krüppel homolog 1* (*Kr-h1*). In *Tribolium*, *HDAC1* knockdown prevents larval-to-pupal transition via derepressing *Kr-h1* expression, thereby influencing JH actions and thus halting metamorphosis. When dsRNA concentration was decreased to 0.01 µg/µl, a very small number of individuals developed to pupal (3/44) and adult (2/44) stages (Table S1) amenable to phenotyping. In marked contrast, RNAi targeting *HDAC 3*, *4*, *6*, or *11* resulted in mortalities ranging from 16.7% to 86.7% depending on dosage and permitted more nuanced and quantitative analysis of phenotypic effects (Table S1). Because no observable phenotypes were found following $HDAC6^{RNAi}$ or $HDAC11^{RNAi}$ even at high dsRNA dosage, we focus on *HDAC 1*, *3*, and *4* in the remainder.

HDACs function during appendage development

To determine affected traits, we measured the scaling relationship of each trait to the cubic root of pupal mass as a proxy of body size since the more commonly used measure of thorax width was affected by *HDAC3* knockdown (treatment: $P < 0.001$, Table S3). $HDAC1^{RNAi}$ resulted in

curtailment of both forewing (i.e. elytra) and hindwing at the pupal stage, which was retained into the adult (Fig. 2D). Similarly, both *HDAC3* or *HDAC4* knockdown diminished wing size (Fig. 2E and F). Thus, *HDAC 1, 3,* and *4* appear to regulate wing development in similar ways. RNAi targeting *HDAC3* and *HDAC4* also affected femur development, but specific effects diverged. *HDAC4*^{RNAi} led to a reduction in femur length (treatment: $P < 0.001$, Table S3) while the slope of the body size/femur length allometry was decreased in *HDAC3*^{RNAi} animals (treatment: $P = 0.163$; treatment × body size: $P = 0.004$, Fig. 2H, Fig. 4A, and Table S3). In contrast, whereas *HDAC3*^{RNAi} increased femur width compared to control individuals (treatment: $P < 0.001$, Table S3), the same measure was reduced in *HDAC4* knockdown animals (treatment: $P = 0.001$, Fig. 2H, Fig. 4B, and Table S3). Lastly, we found that knockdown of *HDAC3* also affected the development of the male reproductive organ, the aedeagus, itself composed of the more proximal phallobase and the more distal parameres. Specifically, genital width increased and attained a more rounded shape at the pupal stage (treatment: $P < 0.001$, Fig.2I and J, Fig. 4C, and Table S3), while adult genitalia exhibited a deformation and overall shortening of both parameres and phallobase, which combined yielded a shortening of overall aedeagus length across all body sizes (treatment: $P < 0.001$, Fig. 2L, Fig. 4D, and Table S3).

***HDACs* function during thoracic and head horns formation**

Head and thoracic horns are textbook examples of evolutionary novelties, and we sought to determine whether *HDAC* function may have been co-opted during the evolution of one or both horn types. *HDAC1*^{RNAi} resulted in a reduction in thoracic horn length and a split tip at the pupal stage (Fig. 3C), whereas the corresponding area in the adult exhibited a broad indentation (compared to the normally smoothly convex outline observed in wildtype or buffer control injected individuals) and small bilateral projections at the respective edge of the indentation (Fig. 3F and G). Effects on head horns could not be quantified with certainty due to the high degree of natural variability of the trait and the very low number of surviving males, which in addition were too small to develop fully formed head horns. However, *HDAC3* knockdown caused measurable shape and scaling changes in thoracic horns. Specifically, *HDAC3*^{RNAi} increased pupal thoracic horn width (treatment: $P < 0.001$, Fig. 4E and Table S4), but decreased pupal thoracic horn length (treatment: $P < 0.001$, Fig. 4F and Table S4). In addition, we found a bilateral indentation to the distal region of the thoracic horn, causing the thoracic horns of large (high nutrition) *HDAC3*^{RNAi} pupae to attain a more conical shape (Fig. 3B). In contrast to thoracic horn phenotypes, *HDAC3*^{RNAi} yielded drastically enlarged head horns, in particular with respect to head horn *width* across the entire range of male body sizes (Fig. 3E, H-K, and Fig. S2).

However, due to the highly varied nature of this phenotypes we were unable to arrive at reliable landmarks for quantitative measure, hence this observation could only be made qualitatively. To determine whether head horn length was also affected, we further measured the scaling relationship of head horn length to body size. *HDAC3*^{RNAi} steepened the slope of the head horn length allometry at both pupal (treatment: P = 0.025, Fig. 4G and Table S4) and adult stages (treatment: P = 0.012, Fig. 4H and Table S4). Notably, *HDAC3*^{RNAi} also reduced maximum asymptotic horn length in adults (treatment: P < 0.001, Fig. 4H and Table S4), which was not detected at the pupal stage (treatment: P = 0.107, Fig. 4G and Table S4). The quantification of head horn length reduction from pupa to adult further confirms this observation (treatment: P < 0.05, Table S3), and this effect was enhanced with increasing body size (treatment × body size effect: P = 0.010, Fig. 4I and Table S3). These results suggest that *HDAC3*^{RNAi} affects head horn *width* during the horn growth phase (which takes place during the larval–to–pupal transition), but affects horn *length* during the pupal remodeling phase of ontogeny. *HDAC4*^{RNAi} in turn not only decreased maximum asymptotic horn length in adults (treatment: P = 0.027, Table S4), but also altered the threshold body size of sigmoidal allometry separating small hornless from large and fully horned males, such that large head horns now also presented in males of relatively small body sizes (treatment: P < 0.001, Fig. 4H and Table S4). In contrast, we did not find abnormal phenotypes with respect to thoracic horns in *HDAC4*^{RNAi} individuals.

The significance of *HDACs* in horned beetle development and evolution

Earlier work on the broad-horned flour beetle *Gnathoceros cornutus* was the first to document a role of *HDACs* in the regulation of nutrition-responsive plasticity in insects (Ozawa et al. 2016). Contrary to its common name, this species does not possess horns but instead exhibits enlarged mandible development in large males. Specifically, *HDAC1*^{RNAi} reduced mandible size in adults, whereas *HDAC3*^{RNAi} led to hypertrophy. Opposite effects were observed with respect to wing size, yet none in genitalia. Collectively, these results were the first to suggest that *HDACs* operate in a module-specific manner to control wing development and sexually dimorphic mandible formation. Our results presented here further confirm that *HDACs* function in an *HDAC*-specific manner in the regulation of appendage size, but also differ in important aspects. First, we find that *HDAC3* plays a critical role in the proper formation of male genitalia, thereby documenting *HDAC* function even in traits generally assumed to be nutrition-insensitive. Second, we show that the precise nature and direction of *HDAC*^{RNAi} effects on appendage formation have diverged between *Gnathoceros* and *Onthophagus* beetles: for example, in *Onthophagus HDAC1*, *3*, and *4* all appear to affect wing size similarly, whereas in *Gnathoceros*

HDAC1^{RNAi} and *HDAC3*^{RNAi} yield opposite effects. Likewise, in *Onthophagus HDAC3*^{RNAi} increased femur width, but *HDAC4*^{RNAi} decreased it, whereas in *Gnathoceros* leg morphology was generally unaffected. Moreover, *HDAC1*^{RNAi} induced developmental arrest at the pre-pupal stages, which is also found in *T. castaneum* (George et al. 2019). However, this phenotype is not observed in *Gnathoceros* (Ozawa et al. 2016). Lastly, our results document a recruitment of *HDAC* function into the formation of an evolutionarily novel structure - head horns - suggesting that *HDAC* function is not just evolutionarily labile among conserved insect traits but also contributed to the comparatively recent evolution of *Onthophagus* weaponry, including the regulation of size, shape, and key components of scaling.

Chromatin modifications and developmental plasticity

This work is the first to implicate chromatin modifications in the regulation of development and plasticity in horned dung beetles. While earlier work documented the existence of the complete methylation machinery in the *O. taurus* genome alongside sex- and nutrition-dependent differences in methylation signatures, the functional significance of chromatin modifications, if any, had remained unknown (Choi et al. 2010; Snell-Rood and Moczek 2013). We now show that downregulation of *HDAC3* and *HDAC4* affect critical aspects of horn formation including size, shape, and the location of the inflection point separating alternate male morphs. Parallel work has now also begun to document chromatin remodeling using sequencing approaches such as ATAC-seq (Assay for Transposase-Accessible Chromatin using sequencing) coupled with RNA-sequencing (Davidson and Moczek, in review). Among others, this work now shows that chromatin remodeling is pervasive during *Onthophagus* development, highly responsive to both nutrition and sex, and often occuring in genome regions containing the binding sites of many known regulators of horn formation (Davidson and Moczek, in review). Future work will need to explore if and how *HDAC* functions may be contributing to these genome-wide remodeling patterns, and more generally the roles of *cis*-regulatory elements in the development and evolution of plasticity in insects.

MATERIALS AND METHODS

Animals

Adult *O. taurus* were collected, courtesy of John Allen, from Paterson Farm near Ravenswood, Western Australia, in 2018. A laboratory population was maintained at 25°C in a sand/soil mixture and fed cow manure twice a week. Larvae used for injection were collected and prepared as described previously (Shafiei et al. 2001).

Identification of O. taurus orthologs for HDACs

The *Onthophagus* orthologs of HDAC genes were identified via reciprocal BLAST to *T. castaneum*, *G. cornutus*, *Drosophila melanogaster*, and *Homo sapiens* in NCBI databases. Amino acid sequences of *HDAC* genes from the above species were aligned with ClustalW algorithm implemented in MEGA X (Kumar et al. 2018). Neighbor-Joining trees were constructed using MEGA X.

Double-stranded RNA (dsRNA) synthesis and injection

Total RNA was extracted with RNeasy Mini Plus Kit (QIAGEN) and reverse transcribed with iScript cDNA Synthesis kit (Bio-Rad). Partial fragments of each genes were amplified with PCR by using gene-specific primers and cloned into pCR4-TOPO TA vector (Invitrogen, Thermo Fisher Scientific). DNA templates for *in vitro* transcription were produced with PCR by using TOPO RNAi primer (Supplementary table S2) (Philip and Tomoyasu 2011). PCR products were purified and concentrated using the QIAquick PCR Purification kit (QIAGEN) and subjected to *in vitro* transcription (MEGAscript T7 Transcription Kit, Thermo Fisher Scientific) and dsRNA purification (MEGAclear Transcription Clean-Up Kit, Thermo Fisher Scientific), according to the manufacturer's protocol. DsRNA was quantified and stored at -80°C until use. Injection was carried out at the early stage of the last larval instar (i.e. the third larval instar, L3). Control animals were injected with injection buffer and kept at the same condition as dsRNA injected animals (See Supplementary table S1 for detailed injection information).

Effect of HDAC3- and HDAC4-RNAi on the scaling relationships between several morphological traits and body size

Since the usual measure of *Onthophagus* body size - thorax width (e.g. Casasa and Moczek 2018; Macagno et al. 2021) - was clearly affected by our RNAi treatments (Fig. 3B and Table S3), we measured the cube root of pupal mass as a proxy for individual body size (Marchini et

al. 2014; Fleming et al. 2021). We used t-tests to compare body sizes between each RNAi-treated and control group.

Consistent with previous studies we analyzed nonlinear horn allometries using untransformed data (e.g. Casasa and Moczek 2018; Macagno et al. 2021). We used the package drc (Ritz et al. 2015) in R 3.5.2 (R Core Team 2018) to fit the body size/head horn length distribution a four-parameter log-logistic (Hill) function in the form

$$y = c + \frac{d-c}{1+\exp(b(\log(x)-\log(a))},$$

with x = body size, y = head horn length, a = body size at the point of inflection of the sigmoid curve, b = slope of the curve, c = minimum and d = maximum asymptotic horn lengths (Macagno et al. 2021). We then inferred whether a complex model including a sigmoidal regression per treatment (i.e. control and RNAi treatments) fitted our data better than a simpler model with one sigmoidal regression including the whole sample by means of the Akaike Information Criterion (AIC) (Akaike 1974). The AIC measures relative model fit - the lower its value, the better the model fits to the experimental data (Burnham et al. 2011). Upon finding the complex model more fitting, we used Welch's t-tests (with Holm-Bonferroni sequential correction where applicable) to compare parameter means (*a*, *b*, *c*, *d*) between control-injected and RNAi treatment groups (Moczek et al. 2002; Casasa and Moczek 2018). We compared control individuals to *HDAC3*^{RNAi} and *HDAC4*^{RNAi} individuals in the case of the adult horn allometry. As for pupal horn allometry, we compared *HDAC3*^{RNAi} to control individuals.

To inspect the effect of RNAi manipulations on all other morphological traits, we modeled trait size as a function of body size, treatment (*HDAC3*^{RNAi} or *HDAC4*^{RNAi} vs control-injected) and their interaction using general linear models in SPSS Statistics 25 (IBM Corp., 2017). Models were simplified by removing non-significant interactions. Data were log-transformed prior to analyses (Huxley 1924). The reduction in horn size during metamorphosis (defined as pupal horn length - adult horn length) was analyzed similarly with a general linear model, using untransformed data as in other analyses of horn morphology. Statistics for morphometric analyses are provided in Supplementary Table S3 and Table S4.

Image Processing

All images were captured with a digital camera (Scion) mounted to a dissecting microscope (Leica MZ16, Germany). Brightness and contrast of images were adjusted across the entire image with Adobe Photoshop CC 2017 (Adobe, USA).

Data accessibility

All data are available in the manuscript and supplementary materials.

Authors' contributions

Y.H. conceived the initial idea, Y.H. and A.P.M. designed the research, Y.H. and J.R.C. performed the experiments, Y.H. and A.L.M.M. analyzed the data, Y.H., A.P.M., and A.L.M.M. wrote the manuscript with contribution from J.R.C.

Competing interests

All authors declare no competing interests.

Funding

Support for this study was provided by awards from the National Science Foundation (IOS1256689) and John Templeton Foundation (61369) to APM. Additional support was provided by the National Natural Science Foundation of China and a Natural Science Foundation of Chongqing for Distinguished Young Scholars award to YH (CSTB2022NSCQ-JQX0025). The opinions, interpretations, conclusions and recommendations are those of the authors and are not necessarily endorsed by the National Science Foundation, the John Templeton Foundation, the National Natural Science Foundation of China, or the Natural Science Foundation of Chongqing.

Acknowledgements

We would like to thank Kayla Copper and Levi Burdine for help with beetle care, and Patrick Rohner for discussion of statistical analyses.

References

Akaike H. 1974. A new look at the statistical model identification. *IEEE Trans. Autom. Control* 19:716–723.

Andersen DS, Colombani J, Léopold P. 2013. Coordination of organ growth: principles and outstanding questions from the world of insects. *Trends Cell Biol.* 23:336–344.

Burnham KP, Anderson DR, Huyvaert KP. 2011. AIC model selection and multimodel inference in behavioral ecology: some background, observations, and comparisons. *Behav. Ecol. Sociobiol.* 65:23–35.

Casasa S, Moczek AP. 2018. Insulin signalling's role in mediating tissue-specific nutritional plasticity and robustness in the horn-polyphenic beetle Onthophagus taurus. *Proc. R. Soc. B Biol. Sci.* 285:20181631.

Casasa S, Schwab DB, Moczek AP. 2017. Developmental regulation and evolution of scaling: novel insights through the study of Onthophagus beetles. *Curr. Opin. Insect Sci.* 19:52–60.

Chen HP, Zhao YT, Zhao TC. 2015. Histone deacetylases and mechanisms of regulation of gene expression. *Crit. Rev. Oncog.* 20:35–47.

Choi J-H, Kijimoto T, Snell-Rood E, Tae H, Yang Y, Moczek AP, Andrews J. 2010. Gene discovery in the horned beetle Onthophagus taurus. *BMC Genomics* 11:703.

Cui J, Lin K, Xu L, Yue F, Yu L, Zhang Q. 2022. Transcriptome Analysis of Beet Webworm Shows That Histone Deacetylase May Affect Diapause by Regulating Juvenile Hormone. *Insects* 13:835.

Davidson PL, Moczek AP. Genome evolution and divergence in cis-regulatory architecture underlie condition-responsive development in horned dung beetles. (In review)

Eberhard WG. 2009. Static Allometry and Animal Genitalia. *Evolution* 63:48–66.

Emlen DJ, Warren IA, Johns A, Dworkin I, Lavine LC. 2012. A mechanism of extreme growth and reliable signaling in sexually selected ornaments and weapons. *Science* 337:860–864.

Fitzsimons HL, Schwartz S, Given FM, Scott MJ. 2013. The Histone Deacetylase HDAC4 Regulates Long-Term Memory in Drosophila. *PLOS ONE* 8:e83903.

Fleming MJ, Carter AW, Sheldon KS. 2021. Dung beetles show metabolic plasticity as pupae and smaller adult body size in response to increased temperature mean and variance. *J. Insect Physiol.* 131:104215.

Frankel S, Woods J, Ziafazeli T, Rogina B. 2015. RPD3 histone deacetylase and nutrition have distinct but interacting effects on Drosophila longevity. *Aging* 7:1112–1129.

George S, Gaddelapati SC, Palli SR. 2019. Histone deacetylase 1 suppresses Krüppel homolog 1 gene expression and influences juvenile hormone action in Tribolium castaneum. *Proc. Natl. Acad. Sci.* 116:17759–17764.

368 George S, Palli SR. 2020a. Histone deacetylase 3 is required for development and metamorphosis in the
369 red flour beetle, Tribolium castaneum. *BMC Genomics* 21:420.

370 George S, Palli SR. 2020b. Histone Deacetylase 11 Knockdown Blocks Larval Development and
371 Metamorphosis in the Red Flour Beetle, Tribolium castaneum. *Front. Genet.* 11:683.

372 Gotoh H, Miyakawa H, Ishikawa A, Ishikawa Y, Sugime Y, Emlen DJ, Lavine LC, Miura T. 2014.
373 Developmental Link between Sex and Nutrition; doublesex Regulates Sex-Specific Mandible
374 Growth via Juvenile Hormone Signaling in Stag Beetles. *PLOS Genet.* 10:e1004098.

375 Hu Y, Linz DM, Moczek AP. 2019. Beetle horns evolved from wing serial homologs. *Science* 366:1004–
376 1007.

377 Huxley JS. 1924. Constant Differential Growth-Ratios and their Significance. *Nature* 114:895–896.

378 Ito Y, Harigai A, Nakata M, Hosoya T, Araya K, Oba Y, Ito A, Ohde T, Yaginuma T, Niimi T. 2013. The role
379 of doublesex in the evolution of exaggerated horns in the Japanese rhinoceros beetle. *EMBO*
380 *Rep.* 14:561–567.

381 Kijimoto T, Moczek AP. 2016. Hedgehog signaling enables nutrition-responsive inhibition of an
382 alternative morph in a polyphenic beetle. *Proc. Natl. Acad. Sci.* 113:5982–5987.

383 Kijimoto T, Moczek AP, Andrews J. 2012. Diversification of doublesex function underlies morph-, sex-,
384 and species-specific development of beetle horns. *Proc. Natl. Acad. Sci.* 109:20526–20531.

385 Koh I, Lee MS, Lee NJ, Park KW, Kim KH, Kim H, Rhyu IJ. 2005. Body size effect on brain volume in Korean
386 youth. *Neuroreport* 16:2029–2032.

387 Kumar S, Stecher G, Li M, Knyaz C, Tamura K. 2018. MEGA X: Molecular Evolutionary Genetics Analysis
388 across Computing Platforms. *Mol. Biol. Evol.* 35:1547–1549.

389 Lafuente E, Beldade P. 2019. Genomics of Developmental Plasticity in Animals. *Front. Genet.* 10:720.

390 Macagno ALM, Edgerton TJ, Moczek AP. 2021. Incipient hybrid inferiority between recently introduced,
391 diverging dung beetle populations. *Biol. J. Linn. Soc.* 132:931–944.

392 Marchini M, Sparrow LM, Cosman MN, Dowhanik A, Krueger CB, Hallgrimsson B, Rolian C. 2014. Impacts
393 of genetic correlation on the independent evolution of body mass and skeletal size in mammals.
394 *BMC Evol. Biol.* 14:258.

395 Moczek A, Hunt J, Emlen D, Simmons L. 2002. Threshold Evolution in Exotic Populations of a Polyphenic
396 Beetle. *Evol. Ecol. Res.* 4:587–601.

397 Moczek AP. 1998. Horn polyphenism in the beetle Onthophagus taurus: larval diet quality and plasticity
398 in parental investment determine adult body size and male horn morphology. *Behav. Ecol.*
399 9:636–641.

400 Moczek AP. 2005. The Evolution and Development of Novel Traits, or How Beetles Got Their Horns.
401 *BioScience* 55:937–951.

402 Moczek AP. 2006. Pupal Remodeling and the Development and Evolution of Sexual Dimorphism in
403 Horned Beetles. *Am. Nat.* 168:711–729.

404 Moczek AP, Cruickshank TE, Shelby A. 2006. When Ontogeny Reveals What Phylogeny Hides: Gain and
405 Loss of Horns During Development and Evolution of Horned Beetles. *Evolution* 60:2329–2341.

406 Mukherjee K, Fischer R, Vilcinskas A. 2012. Histone acetylation mediates epigenetic regulation of
407 transcriptional reprogramming in insects during metamorphosis, wounding and infection. *Front.*
408 *Zool.* 9:25.

409 Müller GB, Wagner GP. 1991. Novelty in Evolution: Restructuring the Concept. *Annu. Rev. Ecol. Syst.*
410 22:229–256.

411 Okada Y, Katsuki M, Okamoto N, Fujioka H, Okada K. 2019. A specific type of insulin-like peptide
412 regulates the conditional growth of a beetle weapon. *PLOS Biol.* 17:e3000541.

413 Ozawa T, Mizuhara T, Arata M, Shimada M, Niimi T, Okada K, Okada Y, Ohta K. 2016. Histone
414 deacetylases control module-specific phenotypic plasticity in beetle weapons. *Proc. Natl. Acad.*
415 *Sci. U. S. A.* 113:15042–15047.

416 Philip BN, Tomoyasu Y. 2011. Gene Knockdown Analysis by Double-Stranded RNA Injection. In: Orgogozo
417 V, Rockman MV, editors. Molecular Methods for Evolutionary Genetics. Methods in Molecular
418 Biology. Totowa, NJ: Humana Press. p. 471–497.

419 R Core Team. 2018. R: A language and environment for statistical computing. Available from:
420 https://www.R-project.org

421 Ritz C, Baty F, Streibig JC, Gerhard D. 2015. Dose-Response Analysis Using R. *PloS One* 10:e0146021.

422 Rohner PT, Hu Y, Moczek AP. 2022. Developmental bias in the evolution and plasticity of beetle horn
423 shape. *Proc. R. Soc. B Biol. Sci.* 289:20221441.

424 Schlichting C, Pigliucci M. 1998. Phenotypic Evolution: A Reaction Norm Perspective. Sinauer

425 Shafiei M, Moczek AP, Nijhout HF. 2001. Food availability controls the onset of metamorphosis in the
426 dung beetle Onthophagus taurus (Coleoptera: Scarabaeidae). *Physiol. Entomol.* 26:173–180.

427 Snell-Rood EC, Moczek AP. 2012. Insulin Signaling as a Mechanism Underlying Developmental Plasticity:
428 The Role of FOXO in a Nutritional Polyphenism. *PLOS ONE* 7:e34857.

429 Snell-Rood EC, Moczek AP. 2013. Horns and the role of development in the evolution of beetle contests.
430 In: Hardy ICW, Briffa M, editors. Animal Contests. Cambridge: Cambridge University Press. p.
431 178–198.

432 Spannhoff A, Kim YK, Raynal NJ-M, Gharibyan V, Su M-B, Zhou Y-Y, Li J, Castellano S, Sbardella G, Issa J-
433 PJ, et al. 2011. Histone deacetylase inhibitor activity in royal jelly might facilitate caste switching
434 in bees. *EMBO Rep.* 12:238–243.

435 Suzuki R, Yaguchi H, Maekawa K. 2019. Histone modifying genes are involved in the molting period
436 during soldier differentiation in Zootermopsis nevadensis. *J. Insect Physiol.* 117:103892.

437 West-Eberhard MJ. 2003. Developmental Plasticity and Evolution. Oxford University Press

438 Xu H-J, Xue J, Lu B, Zhang X-C, Zhuo J-C, He S-F, Ma X-F, Jiang Y-Q, Fan H-W, Xu J-Y, et al. 2015. Two
439 insulin receptors determine alternative wing morphs in planthoppers. *Nature* 519:464–467.

440 Zhang J-L, Yuan X-B, Chen S-J, Chen H-H, Xu N, Xue W-H, Fu S-J, Zhang C-X, Xu H-J. 2018. The histone
441 deacetylase NlHDAC1 regulates both female and male fertility in the brown planthopper,
442 Nilaparvata lugens. *Open Biol.* 8:180158.

443 IBM Corp (2017). IBM SPSS Statistics for Windows, Version 25.0. Armonk, NY: IBM Corp.

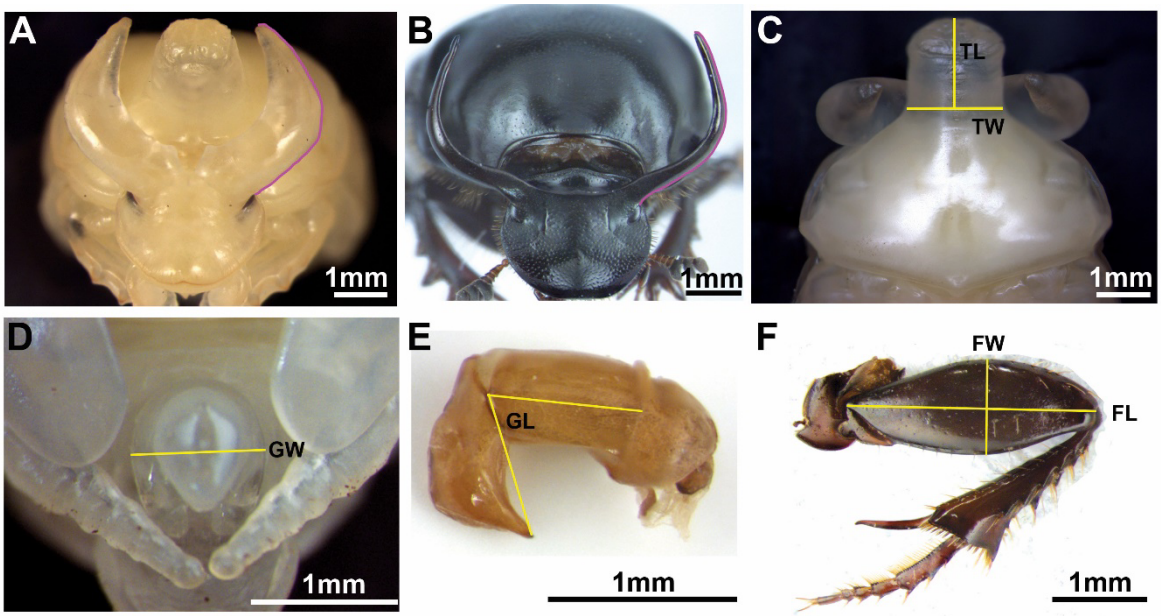

Fig. 1. Wildtype morphology and morphometric landmarks used for morphological quantification. (**A**-**F**) Morphology of the male pupal head (A), male adult head (B), pupal pronotum from dorsal view (C), pupal reproductive organ (D), adult aedeagus (E), and hind leg (F), respectively, and the morphometric landmarks used for measurements (purple and yellow line). TW, thoracic width; TL, thoracic length; GW, genital width; GL, genital length; FL, femur length; FW, femur width.

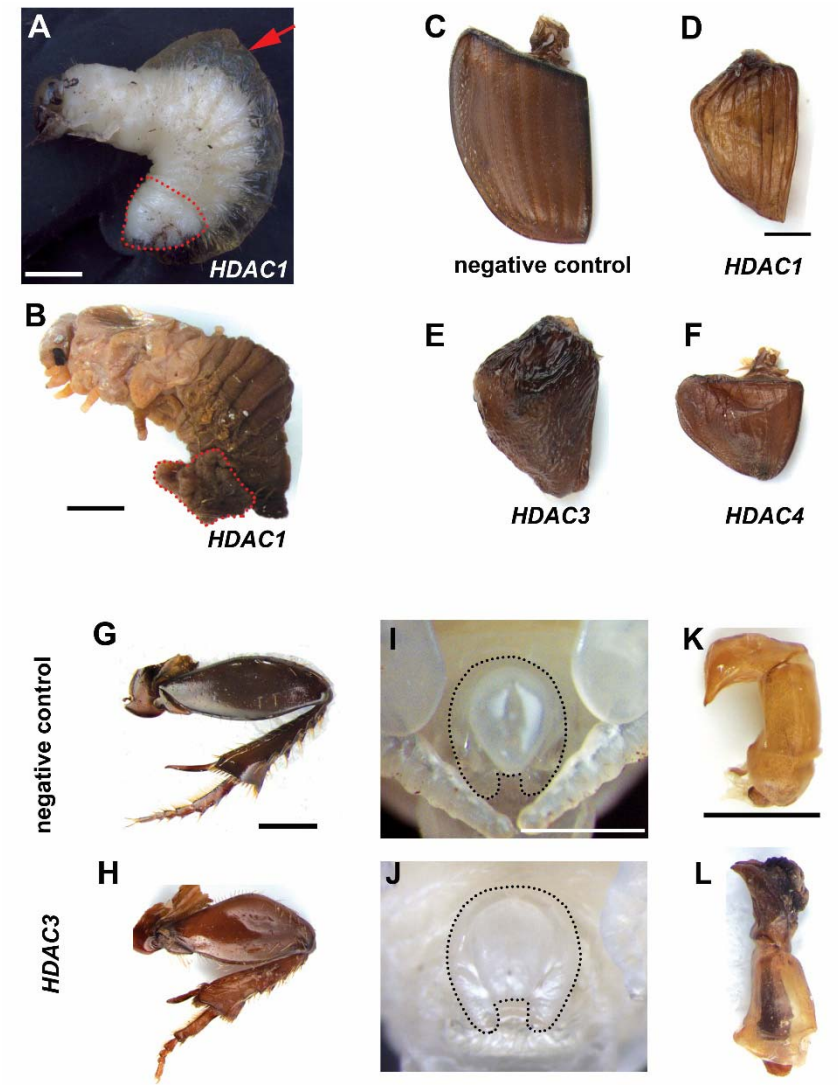

Fig. 2. *HDAC*^{RNAi} effects on molting and appendage development.

(**A** and **B**) Larval-pupal intermediate induced by *HDAC1* knockdown. The fat body accumulated outside of newly-formed pupa is outlined (red dotted line) before (A) and after (B) peeling away the larval cuticle, respectively. Hemolymph in the cavity between larval and newly-formed pupal cuticle is indicated (red arrow in A). (**C**-**F**) Representative wing phenotypes are shown as follows: buffer injection (C), *HDAC1*^{RNAi} (D), *HDAC3*^{RNAi} (E), and *HDAC4*^{RNAi} (F). (**G**-**L**) Morphology of the hind leg (G and H), pupal genitalia (I and J), and adult aedeagus (K and L) compared to buffer injected (third row) and *HDAC3*^{RNAi} (bottom row) individuals, respectively. The RNAi phenotypes and their corresponding negative controls are shown at the same magnification. Scale bars: 1 mm.

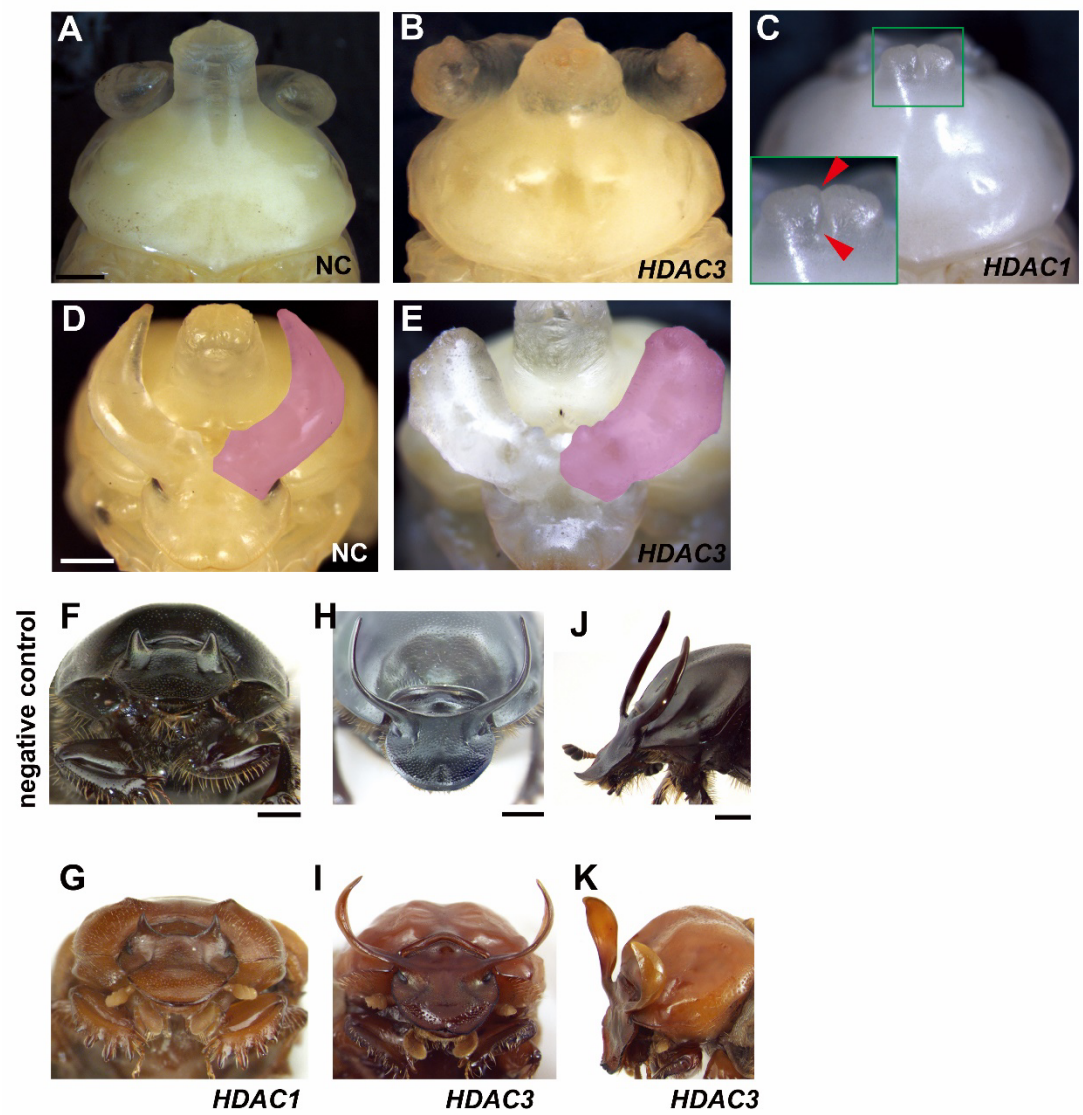

Fig. 3. *HDAC*^{RNAi} effects on thoracic and head horn formation.

(**A**-**C**) The pronotum in negative control (A), *HDAC3*^{RNAi} (B), and *HDAC1*^{RNAi} (C) individuals. Inset in C shows the prothoracic horn. The furrow between paired horn vestiges is indicated by red arrowheads. (**D** and **E**) Representative head horn of negative control (D) and *HDAC3*^{RNAi} (E) individuals, respectively. The right head horn is colored magenta. (**F**-**K**) The morphology of the adult pronotum in front view (F and G), front view of head horns (I and J), as well as head horn viewed from lateral (J and K) in negative control (third row) individuals and following *HDAC* ^{RNAi} (bottom row), respectively. RNAi phenotypes and their corresponding negative controls are shown at the same magnification. Scale bars: 1 mm.

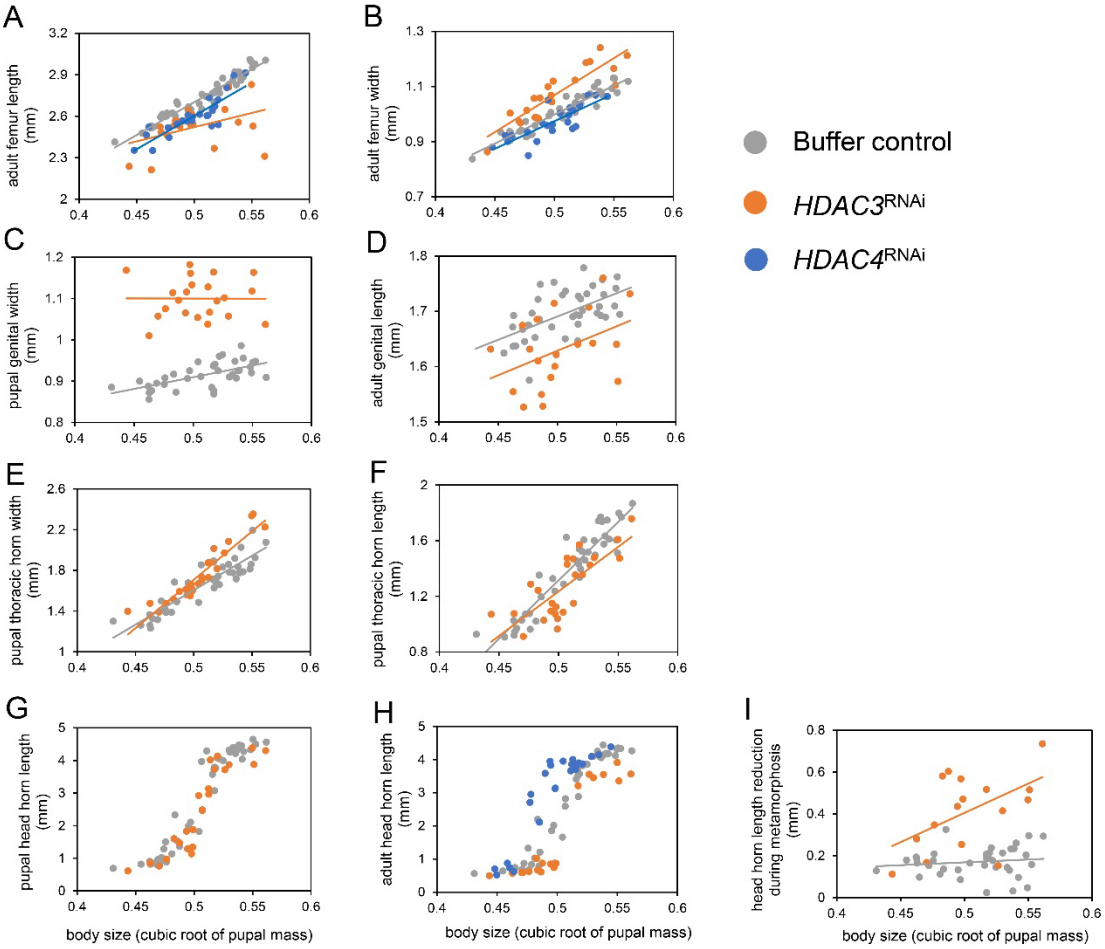

Fig. 4. Effects of *HDAC3* and *HDAC4* knockdown on appendage allometries. (**A** and **B**) Knockdown of *HDAC3* (orange dots) or *HDAC4* (blue dots) on femur length (A) and width (B) compared to buffer-injected control (gray dots). (**C** and **D**) Effects of *HDAC3*^{RNAi} on the male pupal (C) and adult (D) reproductive organ. (**E**-**H**) Changes in thoracic and head horns resulting from *HDAC3*^{RNAi} and *HDAC4*^{RNAi}. (**I**) Reduction in head horn length during the transition from pupa to adult is increased by *HDAC3*^{RNAi} compared to buffer-injections (measured as the difference between pupal head horn length and adult head horn length in the same individual).